PNAS Nexus, 2022, 1, 1–9
https://doi.org/10.1093/pnasnexus/pgac111
Advance access publication date: 11 July 2022
Research Report

Primary cicatricial alopecias are characterized by dysregulation of shared gene expression pathways

Eddy H. C. Wang, Isha Monga, Brigitte N. Sallee, James C. Chen, Alexa R. Abdelaziz, Rolando Perez-Lorenzo, Lindsey A. Bordone and Angela M. Christiano*

Department of Dermatology, Columbia University Irving Medical Center, 1150 St. Nicholas Ave, New York, NY 10032, USA
*To whom correspondence should be addressed: Email: amc65@cumc.columbia.edu
Edited By: David Brenner

Abstract

The primary forms of cicatricial (scarring) alopecia (PCA) are a group of inflammatory, irreversible hair loss disorders characterized by immune cell infiltrates targeting hair follicles (HFs). Lichen planopilaris (LPP), frontal fibrosing alopecia (FFA), and centrifugal cicatricial alopecia (CCCA) are among the main subtypes of PCAs. The pathogenesis of the different types of PCAs are poorly understood, and current treatment regimens yield inconsistent and unsatisfactory results. We performed high-throughput RNA-sequencing on scalp biopsies of a large cohort PCA patients to develop gene expression-based signatures, trained into machine-learning-based predictive models and pathways associated with dysregulated gene expression. We performed morphological and cytokine analysis to define the immune cell populations found in PCA subtypes. We identified a common PCA gene signature that was shared between LPP, FFA, and CCCA, which revealed a significant over-representation of mast cell (MC) genes, as well as downregulation of cholesterogenic pathways and upregulation of fibrosis and immune signaling genes. Immunohistological analyses revealed an increased presence of MCs in PCAs lesions. Our gene expression analyses revealed common pathways associated with PCAs, with a strong association with MCs. The indistinguishable differences in gene expression profiles and immune cell signatures between LPP, FFA, and CCCA suggest that similar treatment regimens may be effective in treating these irreversible forms of hair loss.

Significance Statement:

This study provides valuable insight into the gene expression profiles of major PCA variants, lichen planopilaris (LPP), frontal fibrosing alopecia (FFA), central centrifugal cicatricial alopecia (CCCA), and provides evidence that all three variants share similar pathogenic pathways involving mast cells (MC). These data can be leveraged to design novel therapeutic strategies for PCA patients targeting chlosterogenic pathways, reducing fibrosis, and targeting MCs.

Introduction

Primary Cicatricial Alopecias (PCAs), commonly referred to as scarring alopecias, are a collective group of inflammatory disorders with distinctive pathological features that include the development of fibrosis, permanent destruction of the pilosebaceous unit of the hair follicle (HF), and irreversible hair loss (1). These disfiguring conditions have profound detrimental effects on the psychological health and overall quality of life of affected patients (2–4). The most common PCAs, including Lichen Planopilaris (LPP), Frontal Fibrosing Alopecia (FFA), and Central Centrifugal Cicatricial Alopecia (CCCA), affect mainly women of various demographic groups, and are managed clinically by different treatment regimens. FFA was under-recognized prior to a recent increase in incidence potentially associated with the use of skin care products, leading to the hypothesis that environmental factor(s) may be involved (1, 5). Although LPP, FFA, and CCCA are all classified as PCAs due to the scarring, their clinical presentations are distinct. This common pathogenic feature raises the question that they share underlying molecular pathways.

Studies of PCAs revealed abnormal inflammatory cell infiltrates around the mid HF concentrated around the epithelial stem cell (bulge) region (mixed lymphocytes including Th1, Th2, and mast cells), sebaceous gland, and the infundibulum compartment of the HFs, potentially involving destruction of sebaceous gland, and the development of fibrosis (1, 6–11). This pathological feature is found in all three subtypes of PCAs, therefore, one of the most common initial treatments for PCAs consists of topical and/or intralesional injection of corticosteroids (anti-inflammatory), and oral antibiotics (such as doxycycline for its anti-inflammatory properties) (1, 12, 13). There are also some differential treatments for LPP, FFA, and CCCA that are specific to each subtype. For example PPARg agonists have been used for LPP, but not FFA and CCCA. Hormone modulators are used in FFA patients, but not in LPP (12, 13). These treatments have variable rates of success in slowing the disease process, and are not effective in stimulating

Competing Interest: The authors declare no competing interest.
Received: December 2, 2021. **Accepted:** July 7, 2022

hair regrowth in areas where fibrosis is already present. Thus, it is crucial that the pathobiology of the PCAs is elucidated, to develop new treatment targets for evidence-based randomized clinical trials (12, 13). Genetic studies have been limited and recent GWAS studies on FFA patients revealed susceptibility loci including HLA-B*07:02 (14), whereas a variant in *PADI3* was identified in a subset of CCCA patients that may affect hair shaft formation (15).

Here, we used bulk RNA-sequencing-based (RNAseq) transcriptomics to ask whether there are shared transcriptomic signatures among LPP, FFA, and CCCA and also to determine the degree of association with different immune cell types. We analyzed unique gene expression signatures of each of these PCA subtypes, followed by immunophenotyping techniques and pathway analysis-based methods. Further, we developed an unsupervised clustering training–validation prediction pipeline and supervised machine-learning-based predictive models to classify the PCAs based on the gene expression signatures of LPP, FFA, and CCCA patients. We discovered several core molecular processes among PCAs, which revealed common immunological and mechanistic pathways. The shared pathogenesis suggests unifying molecular mechanisms for therapeutic targeting that could potentially benefit all subtypes of PCA via refined targets and specific immune cell types.

Materials and Methods

Patient demographics

We collected scalp tissue samples from a cohort of 30 LPP, 36 FFA, 9 CCCA patients, and 12 normal controls (NC). A more complete description of our study population, including disease status, treatment history, comorbid conditions, concurrent medications, sex, and age is provided in Table S1 (Supplementary Material).

Ethics statement

All studies were approved by the Institutional Review Board at the Columbia University Irving Medical Center and conducted under the Declaration of Helsinki Principles. Informed consent was received from participants prior to enrollment in the study.

Human biosample collection and processing

A volume of 4 ml punch biopsies were taken from lesional and nonlesional scalp sites as identified by the treating dermatologist. NC samples were donated by healthy volunteers from other studies as part of our normal scalp database. Specimens were fixed in PAXgene Tissue Containers and bisected. One half of the sample was processed for RNA extraction and the other was formalin-fixed and paraffin embedded (FFPE) for immunohistochemistry. Plasma from each subject was preserved for cytokine profiling.

High-throughout RNA-sequencing

RNA extracted from skin biopsies was used for high-throughput bulk RNAseq (GENEWIZ). A standardized RNA-seq pipeline was performed with Illumina HiSeq, 2 × 150 bp (paired-end sequencing with 150 base pairs from each end) and 20 to 30 million reads per sample. PolyA-selection was used to select mRNA and remove rRNA. Briefly, the initial quality control of reads was performed using fastQC and the QC passed Fastq files were used for gene count estimation (transcript per million [TPM]) estimation using Kallisto tool (16) followed by TXTimport (17). All of the samples we submitted for RNAseq met the required quality (RIN score > 7) and amount (> 250 ng). Samples that did not meet this cut-off were not used.

Differential gene expression, pathway analysis, and predictive models

The unique gene hit counts from TXTimport were fed to the downstream differential gene expression (DGE) analysis using *DESeqDataSetFromTximport* function in DESeq2 package in R (18) (Fig. 2B). Utilizing the DGE from bulk RNAseq, we aimed to differentiate the PCAs from NC samples in two ways: (i) PCAs versus NCs and (ii) a multiclass based predictive model to differentiate the different forms of PCA such as (LPP, FFA, and CCCA) versus NCs.

We first implemented an unsupervised training–validation machine learning pipeline on the PCA and NC RNA-seq samples to identify the expression of signature genes associated with each form of PCAs. The training data set (i.e. the cohort used to define an initial novel list of features) consisted of eight NC and nine PCA patients (three LPP and six FFA; Fig. 1B), CCCA patients were not used in the development of the original training dataset. The algorithm was executed without prior information on the diagnosis of individuals (LPP/FFA or NC) to sort all samples based on their raw similarity to/or divergence from each other.

The differentially expressed genes (DEGs) identified in PCAs (alpha = 0.05, *P*-value < 0.05, FDR < 0.05) were validated in the next step by projecting the DEGs onto an independent RNA-seq dataset (14 LPP, 18 FFA, and 12 NC) to ascertain the fidelity of the initial biomarker set in a new set of samples. The validated samples were not used to define the initial signature (Fig. 1C and D). Finally, we applied the biomarker signature to the combined, complete cohort (addition of 16 LPP, 18 FFA, and 9 CCCA) to assess the robustness of the biomarker signature across a total of 30 LPP, 36 FFA, 9 CCCA patients, and 12 NC (Fig. 1E; Figure S2, Supplementary Material). The unsupervised pipeline was able to differentiate PCAs versus NCs, but failed to differentiate between different PCA subtypes.

To classify the different forms of PCAs including LPP, FFA, and CCCA based on gene-expression signatures, we implemented a supervised machine learning pipeline on the transcriptomic profiles of RNAseq datasets. This algorithm was also executed without a priori information on the diagnosis of individuals (LPP/FFA/CCCA or NC) to sort all samples based on their raw similarity to/or divergence from each other. To develop the pipeline, MLSeq (19), an R package with multiple machine learning techniques (MLTs) was used to train the transcriptomic features from RNAseq datasets of PCAs (LPP, FFA, and CCCA) versus NCs. We utilized MLTs such as support vector machines (SVM) and voom-based nearest shrunken centroid (voomNSC). These algorithms are based on the principle of pattern-recognition in the given dataset during training, and predicts the test-set based on these patterns. We used radial basis function (RBF) kernel having kernel width parameter (gamma, *g*) and regularization parameter (c) to build the SVM-based models (see Supplementary Method section 1.7 and Tables S4 and S5 (Supplementary Material) for algorithm details).

Luminex multiplex ELISA and MC tryptase ELISA assay

A comparison of cytokine production from plasma samples from 18 LPP, and 24 FFA patients with a cohort of 10 NCs was performed via a Luminex Multiplex ELISA platform. The Luminex panel is a customized 36-plex array that contains inflammatory cytokines secreted by CD8, Th1, Th2, Th17, and mast cells (ThermoFisher Scientific; Table S3, Supplementary Material). A separate single-analyte ELISA was performed to measure the

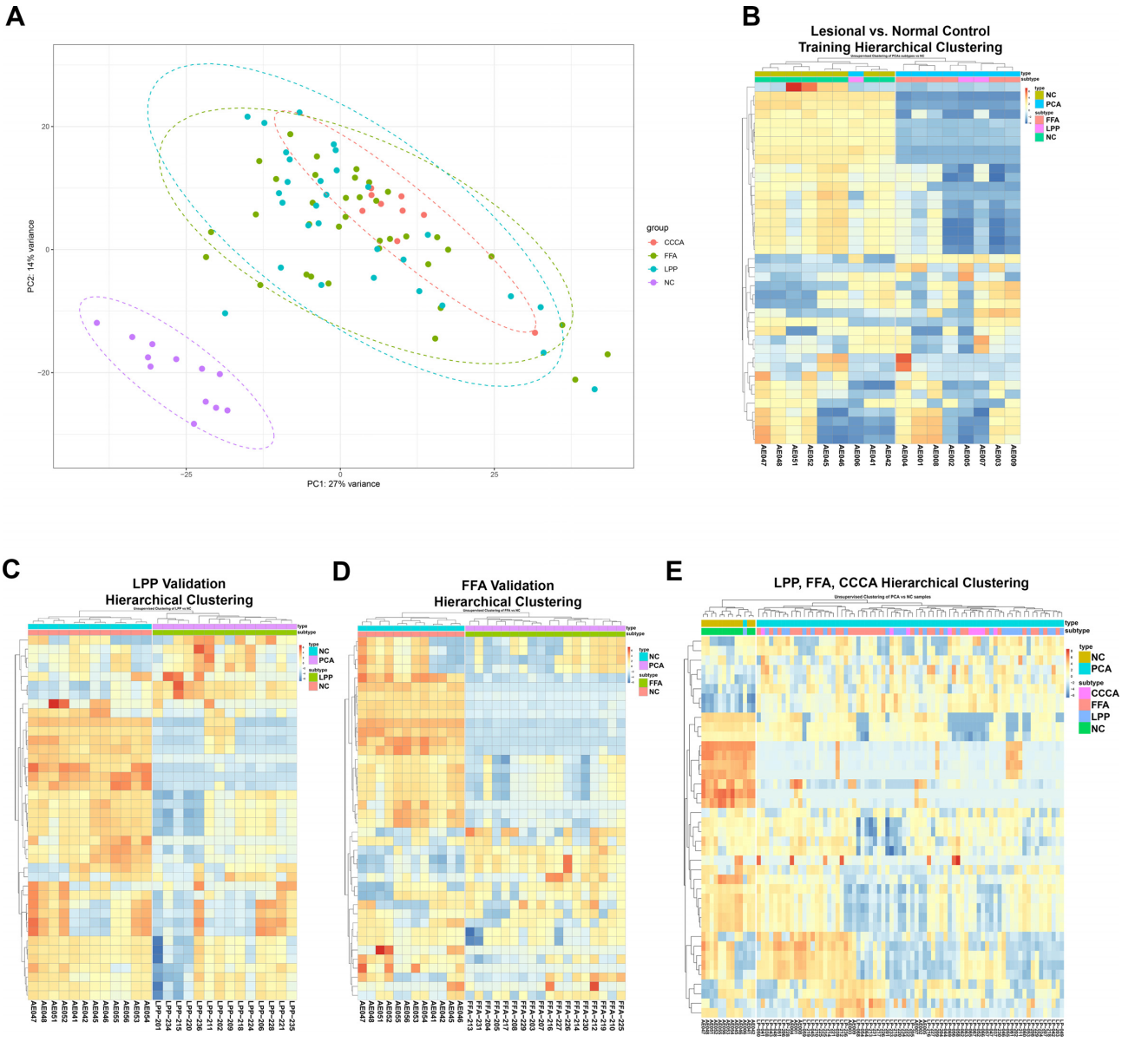

Fig. 1. LPP, FFA, and CCCA share a gene expression profile compared to controls. RNA-seq followed by principal component analysis (PCA) using variance stabilized transformed (VST) values of lesional biopsies from LPP (blue), FFA (green), and CCCA (red), showed no independent clustering, indicating no discernible difference in their transcriptomic profiles while NC biopsies (purple) showed clear segregation from LPP, FFA, and CCCA lesions (A). Identification of unique gene sets representative of LPP and FFA with a training set of three LPP and six FFA lesional biopsies compared to eight NC biopsies (B). This unique gene signature was validated with larger cohorts of LPP (C) ($n = 14$) or FFA (D) ($n = 18$) samples compared to 12 NC samples and showed high reproducibility. The training–validation set workflow is a novel and robust approach to identify or differentiate unique gene signatures of disease entities. When applying the signature to the complete cohort (E) (30 LPP, 36 FFA, 9 CCCA, and 12 NC), we saw no observable differences between PCA subtypes in molecular analysis.

plasma level of mast cell (MC) tryptase (RayBiotech Inc). Luminex assays and MC tryptase ELISA were performed and analyzed by the Columbia Biomarkers Core Laboratory following the manufacturer's protocol.

Histology and immunohistochemistry

Tissue blocks from five LPP, five FFA, five CCCA patients, and five NC were selected for histological and IHC analyses. H&E staining and Toluidine Blue staining was performed following previously established protocols (20). IHC analyses for CD4, CD8, macrophages, dendritic cells, and MCs were performed using the dilutions described in Table S2 (Supplementary Material).

Statistical analysis

DGE analysis was performed using the hit count data and the DESeq2 package in Bioconductor, which estimates variance-mean dependence in count data and tests for differential expression based on a model using the negative binomial distribution. The molecular pathways represented by the DGEs were determined using the TCGAbiolinks package (21) to detect functional enrichment of our gene list based on ontologies and top pathways with FDR < 0.05 displayed.

Immune deconvolution scores were inferred directly from RNAseq data on whole skin biopsies (22). Representative marker transcripts for each immune cell type were quantified for relative differential expression. Scores were created via Fisher's

integration of the differential expression and corresponding *P*-values and the figure arrays these scores in a 2D semi-log graph.

Results

LPP, FFA, and CCCA share an indistinguishable gene expression profile

We first compared the global RNA-seq expression data between LPP, FFA, CCCA, and NC scalp and expected to observe discrete clustering into four groups. Unexpectedly, the overall gene expression profile of all PCA subjects (LPP, FFA, and CCCA) did not show any distinguishable differences and principal component analysis (PCA) did not show any distinct separation of the LPP, FFA, and CCCA cohorts, indicating that differences in gene expression in the scalp was negligible among all PCAs (Fig. 1A). The NC samples formed a distinct cluster away from lesional skin of LPP/FFA/CCCA (Fig. 1A). In addition, we found that the gene expression signatures for LPP, FFA, and CCCA patients were highly similar to each other and robustly separated from the NC subjects (Fig. 1E).

The lack of differences in the gene expression profile is supported by several recent studies that investigated gene expression and histological presentation of LPP, FFA, and CCCA patients (7, 8). The similarity in gene expression profile suggests shared molecular drivers despite differences in the clinical presentation of hair loss among PCAs. Notably, we found that the gene expression profiles in lesional scalp biopsies was highly similar to the corresponding nonlesional scalp biopsies from the same patient (Figures S1A and S5, Supplementary Material).

Training dataset of LPP and FFA revealed a gene signature in separate validation datasets

To classify the LPP, FFA, and CCCA from NCs, we implemented an unsupervised hierarchical clustering algorithm (Fig. 1B), which identified a unique set of genes that were differentially expressed between the lesional PCA samples and NCs (alpha = 0.05, *P*-value < 0.05, and FDR < 0.05). However, unsupervised clustering failed to differentiate the LPP, FFA, and CCCA signatures from one another, which further corroborated our PCA (Fig. 1A).

Using unsupervised clustering, we identified a unique set of genes that were differentially expressed between the lesional PCA samples and unaffected controls from a training data set consisted of eight NC and nine PCA patients (three LPP, six FFA; FDR < 0·05; Fig. 1B). In addition, we found the gene signature for LPP and FFA patients was highly similar and distinctly separated from the NC subjects. When applying the gene signature from the training step to our second cohort of subjects (14 LPP, 18 FFA, and 12 NC), we achieved a high degree of segregation of LPP and FFA patients from NC (Fig. 1C and D). With a combined analysis of the complete cohort (30 LPP, 36 FFA, 9 CCCA, and 12 NC), we still observed a distinct segregation of PCA patients from the NCs while showing no differences among PCA types (Fig. 1E). In these exercises, the training gene expression profile was independently validated in LPP or FFA cohorts separately, reflecting that the algorithm was able to identify and segregate the patient samples from NCs using a single, highly generalizable panel of biomarkers (also supported by unsupervised hierarchical clustering; Figure S2, Supplementary Material). CCCA samples were included in the final combined analysis, since the number of samples was not sufficient for inclusion in both the training and validation analyses. The unsupervised training validation analysis robustly segregated the PCAs from NCs, but did not separate the transcriptomic signatures to classify PCA subtypes.

LPP, FFA, and CCCA gene expression profiles revealed shared molecular pathways

Downregulation of cholesterogenic genes

Our computational analysis revealed a core set of DEGs involved in cholesterol biosynthesis, fatty acid biosynthesis and metabolism pathways (Fig. 2A–C, red bars). These differentially regulated pathways were found when we conducted pathway analysis of lesional skin RNA-seq compared to NC biopsies (FC +/− 1·5, FDR ≤ 0·05). Individual analysis of LPP (Fig. 2A), FFA (Fig. 2B), or CCCA (Fig. 2C) compared to NC showed similar differentially regulated pathways. Notably, the cholesterogenic genes found in these pathways were mainly downregulated in lesional skin, suggesting a decrease of cholesterol biosynthesis, which likely reflects the loss of sebaceous glands and/or decreased sebum production.

Upregulation of fibrotic signature genes

Pathway analysis also revealed upregulation of many genes involved in fibrosis (Fig. 2A and B, green bars), especially for LPP and FFA. These genes are classified under the category of "hepatic fibrosis" by the database of TCGAbiolinks. The development of fibrosis is one of the defining features in PCAs and is postulated to be the cause of permanent loss of HF bulge stem cells (12, 13). The fibrosis pathway in CCCA was also increased, but did not reach statistical significance (not shown). The abundance of fibrotic tissue was corroborated using hematoxylin and eosin (H&E) staining of lesional skin (especially in LPP and FFA), where we observed densely packed extracellular matrix fibers (Fig. 4A).

Over representation of MC signature

To develop a gene expression profile reflecting different immune cells, we previously generated an immunopanel algorithm to deconvolute defined immune cell signatures (23) from RNA-seq performed on whole biopsies (22). We previously validated this algorithm while analyzing the inflammatory infiltrate in alopecia areata (AA), which showed a high $CD8^+$ T cell and Th1 score (24). The differential distribution of each immune cell type is represented in a 2D array comparing the relative consensus differential expression of unique markers and the *P*-value of the differential expression (22). In PCAs, the immunopanel analysis revealed a striking and highly significant MC signature (represented by TPSAB1, MS4A2, and CMA1), in LPP, FFA, and CCCA lesions (Fig. 3A–C) a Th1 signature (CD4, IFNg, STAT4, and IL12). Notably, the *x*-axis (representing *P*-values) is shown in log scale, indicating that each step toward the right of the x-axis represents a 10-fold increase in significance. Thus, the significance of MC score is in the range of log *P*-value = 10^{-11} to 10^{-15}.

Immunohistological analysis of PCAs revealed infiltration with MCs

Immunohistological analysis of PCA biopsies for the presence of immune cells such as CD4/CD8 T cells, macrophages (CD68), and dendritic cells (CD209) showed similar staining patterns between lesional (Fig. 4A) and nonlesional skin (Figure S1B, Supplementary Material). In addition, we observed strong positive staining for MCs (MC tryptase and Toluidine Blue) in LPP, FFA, and CCCA around the sebaceous gland and within fibrotic tissue (Fig. 4A). In contrast, in NC skin, we did not detect a large number of MCs in the bulb and sebaceous gland region, consistent with the overrepresentation of the MC signature in RNAseq in PCAs. We also found positive staining for MHC Class I and II, consistent with the elevated Th1 signature as represented by genes such as IFNg,

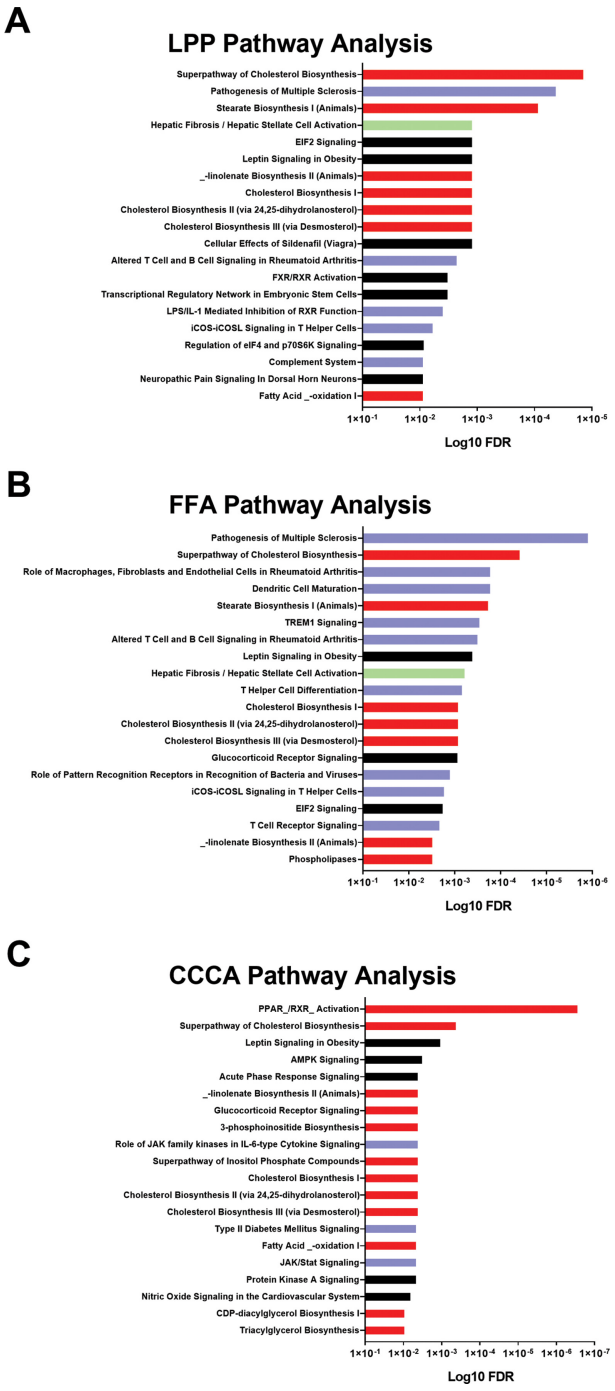

Fig. 2. Pathway analysis of LPP, FFA, and CCCA revealed shared dysregulated pathways in cholesterol biosynthesis and fibrosis. Pathway analysis of significantly DEGs between LPP lesions (A), FFA lesions (B), CCCA lesions alone (C), when compared to NCs. Pathway analysis revealed core shared pathways among LPP, FFA, and CCCA such as pathways involved in fatty acid and cholesterol biosynthesis (red bars) and immune response and signaling (blue bars). Fibrosis pathway is also shared between LPP and FFA (green bar) and CCCA (not shown in top 20). Black bars represent other pathways. Top 20 representative pathways are shown. Analysis was performed with R package TCGA Biolinks with access to The National Cancer Institute (NCI) Genomic Data Commons (GDC).

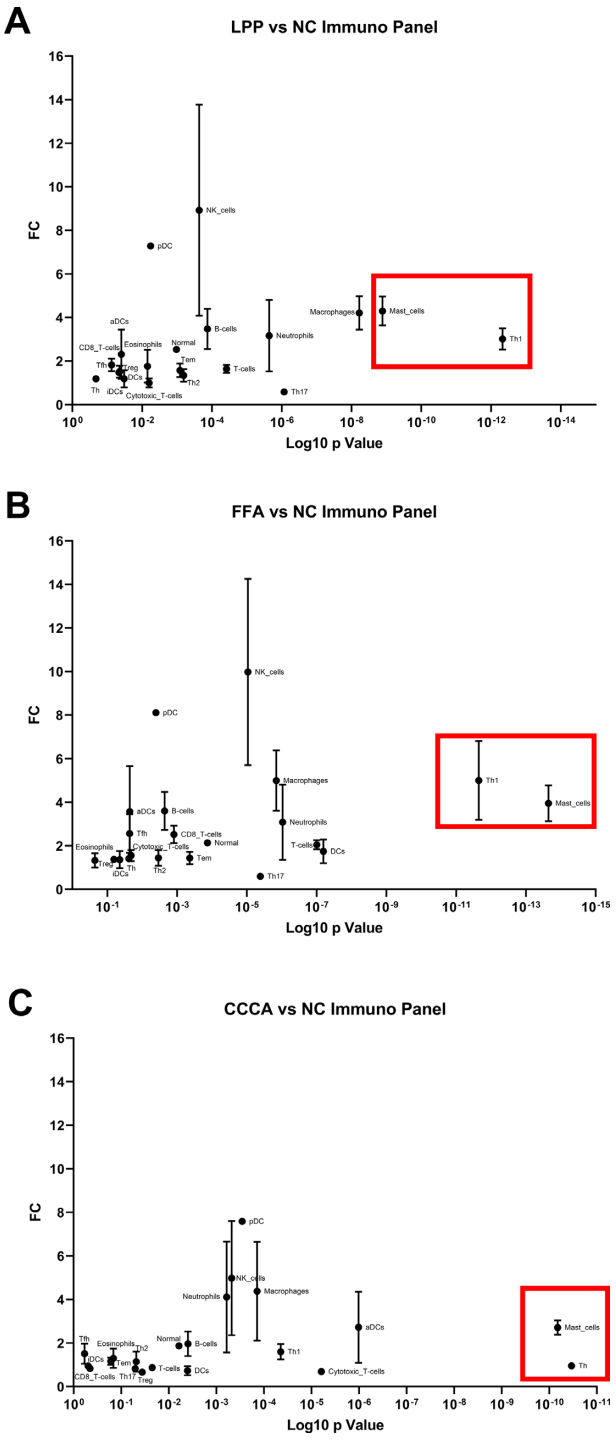

Fig. 3. Deconvolution of immune cells revealed over-representation of MC signature. Immune deconvolution scores were inferred from the RNA-seq data and revealed the association of different immune cells that were not detected by standard pathway analysis. By deconvoluting the immune cell scores, over-representation of a MC signature was identified in LPP lesional skin (A) as well as in FFA (B), and CCCA (C) lesions compared to NC. The x-axis represents log10 of the adjusted P-value (FDR) with each step toward the right represent a 10-fold increase in significance.

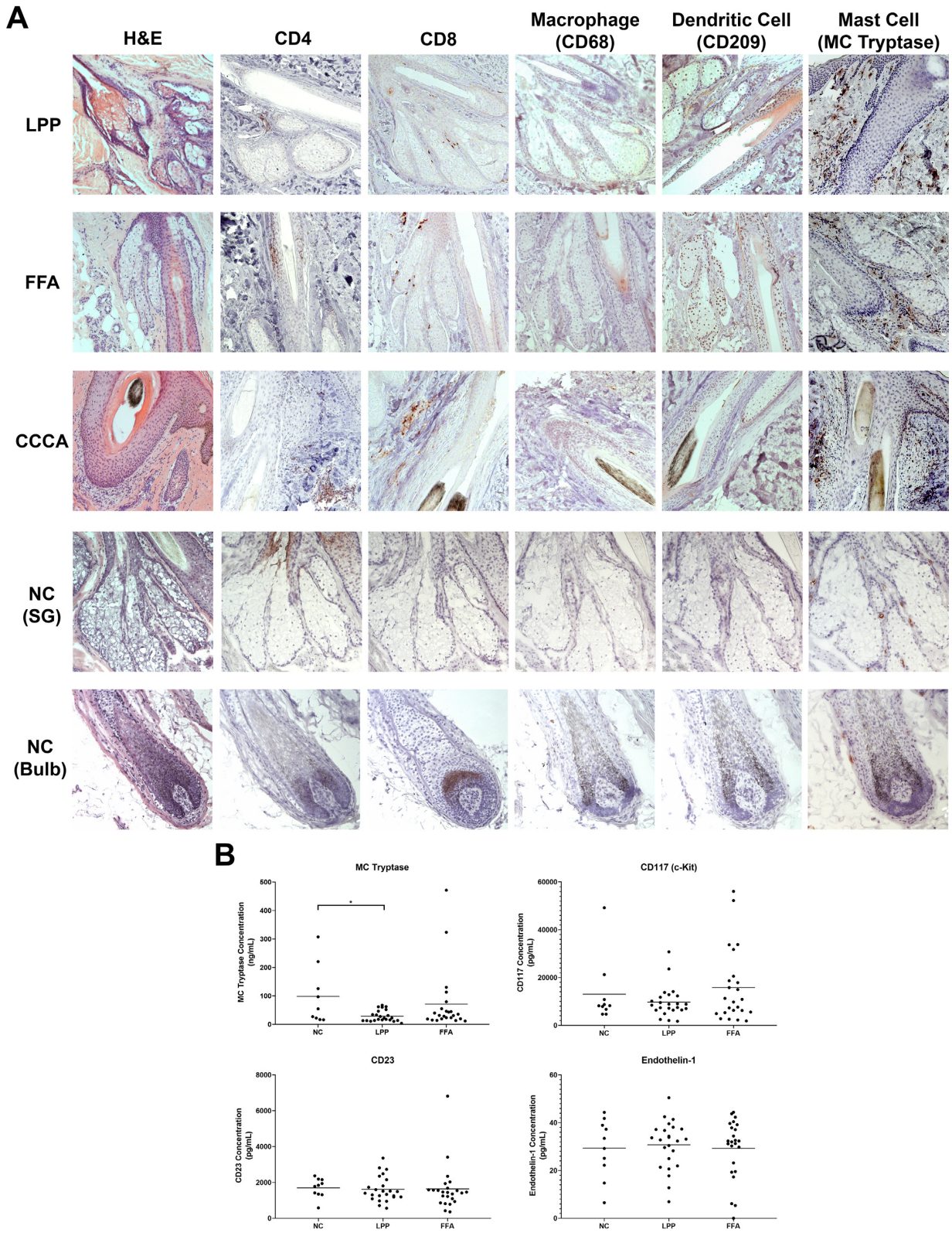

Fig. 4. Presence of MCs by histology and multiplex ELISA. Histological analysis of LPP, FFA, and CCCA skin revealed a high number of MCs in the peri-follicular area of the HFs in PCAs that were not present in NC (A). There were a relatively small number of CD4+ and CD8+ T cells around the sebaceous gland and a very small number of macrophages and dendritic cells in LPP, FFA, and CCCA lesional samples. The inflammatory infiltrates in PCA lesions are found near the sebaceous gland and isthmus region and showed no differences compared to nonlesional skin from the same patient (Figure S1B, Supplementary Material). The plasma level of MC markers (MC tryptase, CD117, CD23, and Endothelin-1) showed no significant difference between NC, LPP, FFA, and CCCA, suggesting MC activation is restricted to the skin (B).

STAT4, and IL12. The presence of sebaceous glands (HSD3B1) was observed (Figure S3, Supplementary Material).

To ask whether involvement of MCs revealed by RNA-seq and IHC analysis extended beyond the skin, we measured the level of tryptase in the plasma of LPP and FFA patients (Fig. 4B). In addition, we performed a multiplex ELISA (Luminex) which included three additional MC markers (CD117, CD23, and Endothelin-1) on plasma samples of 23 LPP, 23 FFA, and 9 NC subjects (Fig. 4B). We found that plasma MC marker levels were similar among the different disease groups, suggesting that MC activity is primarily restricted to the skin and not a systemic feature of PCAs. The levels of additional inflammatory cytokines in plasma are shown in Figure S4 (Supplementary Material). There were no significant differences in the levels of these cytokines among LPP and FFA patients.

Discussion

Previously, it was widely believed that the subtypes of PCA; LPP, FFA, and CCCA were distinct disease entities. However, reports of patients switching PCA phenotypes between clinical subtypes have been reported in the literature, and the histopathology of PCA variants is highly similar (11), suggesting that phenotypic overlap may be driven by shared mechanisms, though these remained undefined.

Our study was driven by an analytic pipeline that has not been implemented in the study of PCAs. Instead of a traditional exploratory gene expression analysis, we first identified a gene signature from an initial cohort of patients (training set), and then validated the association in an independent cohort with a supervised analysis (validation sets). This is the gold-standard validation of machine-learning classification studies, and establishes significant evidence to the robustness of our PCA gene signatures and their association to the disease.

We found striking similarity among the gene signatures in the skin of LPP, FFA, and CCCA, which showed virtually no differences between all three classifications of PCAs. Pathway analyses and immunopanel on these gene signatures revealed changes in three main pathways: (1) cholesterogenesis; (2) fibrosis; and (3) MCs.

Scarring and the development of fibrotic tissue in the skin is one of the distinguishing clinical features of PCAs. Pathway analysis of PCAs showed a strong association of hepatic fibrosis pathway in the lesional skin of LPP and FFA, as well as CCCA to a lesser extent (Fig. 2A and B). ICAM1, MMP2, MMP13, LEP, COL1A1, and COL1A2 are some of the genes involve in the development of fibrosis and are significantly elevated in PCAs. Histologically, fibrotic tissue was also observed around the infundibulum region of the HF, near the sebaceous glands of PCA patient scalp (Fig. 4A). The same fibrosis pathway and histological presentation can be found in LPP, FFA, and CCCA, which further supports a shared mechanism that may lead to permanent hair loss through the replacement of the HF by fibrous tissue.

Our immunohistological analyses also demonstrated a mixed inflammatory infiltrate within and around the sebaceous gland/isthmus region of the HF in PCAs. We located some sebaceous glands in the lesional skin of most PCA patients, since the biopsy site was near the edge of the lesion. However, prominent inflammation was observed around the SGs in both lesional as well as nonlesional skin and the changes in gene expression may precede loss of the sebaceous glands even before overt hair loss is visible.

We observed a significant downregulation of cholesterol biosynthesis genes such as CYP51A1, DHCR7, and MSMO1 in the PCA biopsies. These genes are involved in different stages of cholesterol biogenesis, lipid synthesis and even drug metabolism. The defect in cholesterol biosynthesis may result in accumulation of sterol intermediates which can initiate inflammatory responses (25, 26).

Unexpectedly, we identified a distinct and highly significant MC gene signature in PCA patients, which was subsequently confirmed by a larger patient cohort in the validation dataset and supported by the detection of elevated MC markers by immunohistochemistry. The presence of MCs suggests a possible trigger of innate immune responses in PCA potentially involving allergic mechanisms, in addition to the involvement of Th1 cells, as previously reported in FFA (7). MCs play a key role in inflammation and immediate allergic reaction such as contact with external antigens and allergens (27, 28). The sustained activation of MCs could also result in the development of fibrosis (29, 30), however, the causes of MC activation and its relationship to the development of fibrosis in PCAs invite further investigation.

The potential association of PCAs with environmental triggers has been a focus of several recent studies. The questionnaire-based study focused on FFA patients found a possible association with leave-on facial skin care products, including sunscreens (5, 31). In a study of the main ingredients in sunscreen (such as oxybenzone), the authors found 87 out of 100 products tested contained at least one potential allergen identified in previous patch testing results of FFA patients (32). In a case series study in Brazil involving patch and photopatch testing of 63 FFA patients, 59% of subjects had at least one positive test (33). While it is possible that certain compounds often used in fragrances like Myroxylon pereirae (balsam of Peru) and linalool lhydroperoxide may increase predisposition to allergy and immune-mediated FFA (5), the underlying mechanisms remain to be determined. In our patient cohort, 55% of patients (16/30 LPP, 20/36 FFA, and 0/9 CCCA) self-reported to have allergic reactions or allergy to some substance/allergen (not limited to facial products; Table S1, Supplementary Material). Taken together, these lines of evidence may further support the role of environmental factors such as allergens in the pathogenesis of PCAs.

In addition to their immune functions, MCs have also been implicated in fibrosis, including some skin models such as graft-versus-host disease and wound healing (29, 30), and modulating MC activation may have therapeutic benifits in preventing fibrotic processes (34). A recent study also found a high number IL-17A positive MCs in LPP lesions and suggested autoactivation of the IL-23/IL-17 axis (35).

While there are immune infiltrates around the HF and immune-mediated pathways were observed in our gene expression data, mainstream immune-modulating treatments such as corticosteroids are not always effective in PCAs and may introduce side-effects (12, 13). We recently evaluated the efficacy of JAK inhibitors (36, 37) in PCAs, which resulted in a decrease of LPP activity Index in 8 out of 10 patients (38). Therefore, while JAK inhibition may be a promising treatment for PCAs, further study on the mechanisms of action is required, since MCs are also a target of JAK inhibitors, and JAK inhibitors, such as ruxolitinib, alone can also inhibit MC degranulation (39). Inhibiting JAK–STAT signaling in conjunction with MC stabilizers may be an effective combinatorial regimen in treating PCAs. We also compared the results to another form of inflammatory hair loss condition, AA, we found lesional biopsies have different immunohistological features and gene expression profile as PCA lesions (Figure S6, Supplementary Material).

In summary, we discovered a set of common pathways through gene expression analyses. Immunophenotyping of LPP, FFA, and

CCCA patients revealed a striking presence of MC associated genes. These findings support the potential role of environmental factors such as allergens (such as facial products and sunscreens) in the immunopathogenesis of PCAs. In conjunction with the identification of decreased cholesterogenic genes (decreased sebum production) shared among different PCAs, treatments involving modulation of MCs numbers/activity to reduce fibrosis and/or upregulation of cholesterol biosynthesis pathways invite future clinical investigation to improve clinical outcomes in the treatment of PCAs.

Acknowledgments

We thank Wangyong Zeng for processing the human biosamples, and Katherine Kuang and Stephanie Li for performing the histological analyses. We thank the Department of Systems Biology for their assistance with data analysis.

Supplementary Material

Supplementary material is available at *PNAS Nexus* online.

Funding

This project was funded by the NIH/NIAMS Immunophenotyping of Lichen Planopilaris (1R21AR073013), the NIH/NIAMS Columbia University Skin Disease Resource-Based Center (epiCURE; 1P30AR069632), and private family foundation funding. We thank the JP Sulzberger Columbia University Genome Center for performing RNA-sequencing (NIH/NCI P30 Cancer Center Support grant P30CA013696) and the Columbia Biomarkers Core Laboratory for performing the Luminex assays (NIH/NCATS UL1TR001873).

Authors' Contributions

A.M.C., L.A.B., and E.H.C.W. designed the experiments. L.A.B. and B.N.S. recruited patients and collected biosamples. E.H.C.W., J.C.C., A.R.A., and R.P.L. performed the experiments. J.C.C. and I.M. performed the computational analyses. E.H.C.W., J.C.C., I.M., and A.M.C. interpreted the results. E.H.C.W., A.M.C., L.A.B., B.N.S., and I.M. wrote the manuscript.

Data Availability

RNA-seq data is available on GEO Database with ID GSE186075.

References

1. Harries MJ, Paus R. 2010. The pathogenesis of primary cicatricial alopecias. Am J Pathol. 177(5):2152–2162.
2. Akintilo L, Hahn EA, Yu JMA, Patterson SSL. 2018. Health care barriers and quality of life in central centrifugal cicatricial alopecia patients. Cutis. 102(6):427–432.
3. Alirezaei P, *et al.* 2019. Compared to controls, individuals with lichen planopilaris have more depression, a lower self-esteem, and a lower quality of life. Neuropsychobiology. 78(2):95–103.
4. Saceda-Corralo D, *et al.* 2018. Health-related quality of life in patients with frontal fibrosing alopecia. JAMA Dermatol. 154(4):479–480.
5. Aldoori N, *et al.* 2016. Frontal fibrosing alopecia: possible association with leave-on facial skin care products and sunscreens; a questionnaire study. Br J Dermatol. 175(4):762–767.
6. Aguh C, Dina Y, Talbot CC, Jr., Garza L. 2018. Fibroproliferative genes are preferentially expressed in central centrifugal cicatricial alopecia. J Am Acad Dermatol. 79(5):904–912.e1.
7. Del Duca E, *et al.* 2020. Frontal fibrosing alopecia shows robust T helper 1 and Janus kinase 3 skewing. Br J Dermatol. 183(6):1083–1093.
8. Harries M, Hardman J, Chaudhry I, Poblet E, Paus R. 2020. Profiling the human hair follicle immune system in lichen planopilaris and frontal fibrosing alopecia: can macrophage polarization differentiate these two conditions microscopically?. Br J Dermatol. 183(3):537–547.
9. Harries MJ, *et al.* 2013. Lichen planopilaris is characterized by immune privilege collapse of the hair follicle's epithelial stem cell niche. J Pathol. 231(2):236–247.
10. Imanishi H, *et al.* 2018. Epithelial-to-mesenchymal stem cell transition in a human organ: lessons from lichen planopilaris. J Invest Dermatol. 138(3):511–519.
11. Mirmirani P, *et al.* 2005. Primary cicatricial alopecia: histopathologic findings do not distinguish clinical variants. J Am Acad Dermatol. 52(4):637–643.
12. Bolduc C, Sperling LC, Shapiro J. 2016. Primary cicatricial alopecia: other lymphocytic primary cicatricial alopecias and neutrophilic and mixed primary cicatricial alopecias. J Am Acad Dermatol. 75(6):1101–1117.
13. Bolduc C, Sperling LC, Shapiro J. 2016. Primary cicatricial alopecia: lymphocytic primary cicatricial alopecias, including chronic cutaneous lupus erythematosus, lichen planopilaris, frontal fibrosing alopecia, and Graham-Little syndrome. J Am Acad Dermatol. 75(6):1081–1099.
14. Tziotzios C, *et al.* 2019. Genome-wide association study in frontal fibrosing alopecia identifies four susceptibility loci including HLA-B∗07:02. Nat Commun. 10(1):1150.
15. Malki L, *et al.* 2019. Variant PADI3 in central centrifugal cicatricial alopecia. N Engl J Med. 380(9):833–841.
16. Bray NL, Pimentel H, Melsted P, Pachter L. 2016. Near-optimal probabilistic RNA-seq quantification. Nat Biotechnol. 34(5):525–527.
17. Soneson C, Love MI, Robinson MD. 2015. Differential analyses for RNA-seq: transcript-level estimates improve gene-level inferences. F1000Res. 4:1521.
18. Love MI, Huber W, Anders S. 2014. Moderated estimation of fold change and dispersion for RNA-seq data with DESeq2. Genome Biol. 15(12):550.
19. Goksuluk D, *et al.* 2019. MLSeq: machine learning interface for RNA-sequencing data. Comput Methods Programs Biomed. 175:223–231.
20. Xing L, *et al.* 2014. Alopecia areata is driven by cytotoxic T lymphocytes and is reversed by JAK inhibition. Nat Med. 20(9):1043–1049.
21. Colaprico A, *et al.* 2016. TCGAbiolinks: an R/Bioconductor package for integrative analysis of TCGA data. Nucleic Acids Res. 44(8):e71.
22. Chen JC, Perez-Lorenzo R, Saenger YM, Drake CG, Christiano AM. 2018. IKZF1 enhances immune infiltrate recruitment in solid tumors and susceptibility to immunotherapy. Cell Syst. 7(1):92–103.e4.
23. Bindea G, *et al.* 2013. Spatiotemporal dynamics of intratumoral immune cells reveal the immune landscape in human cancer. Immunity. 39(4):782–795.
24. Chen JC, Cerise JE, Jabbari A, Clynes R, Christiano AM. 2015. Master regulators of infiltrate recruitment in autoimmune disease identified through network-based molecular deconvolution. Cell Syst. 1(5):326–337.

25. Karnik P, *et al.* 2009. Hair follicle stem cell-specific PPARgamma deletion causes scarring alopecia. J Invest Dermatol. 129(5):1243–1257.
26. Panicker SP, *et al.* 2012. Sterol intermediates of cholesterol biosynthesis inhibit hair growth and trigger an innate immune response in cicatricial alopecia. PLoS ONE. 7(6):e38449.
27. Amin K. 2012. The role of mast cells in allergic inflammation. Respir Med. 106(1):9–14.
28. Dudeck A, *et al.* 2011. Mast cells are key promoters of contact allergy that mediate the adjuvant effects of haptens. Immunity. 34(6):973–984.
29. Claman HN, Jaffee BD, Huff JC, Clark RA. 1985. Chronic graft-versus-host disease as a model for scleroderma. II. Mast cell depletion with deposition of immunoglobulins in the skin and fibrosis. Cell Immunol. 94(1):73–84.
30. Willenborg S,, *et al.* 2014. Genetic ablation of mast cells redefines the role of mast cells in skin wound healing and bleomycin-induced fibrosis. J Invest Dermatol. 134(7): 2005–2015.
31. Cranwell WC, Sinclair R. 2019. Frontal fibrosing alopecia: regrowth following cessation of sunscreen on the forehead. Australas J Dermatol. 60(1):60–61.
32. Marks DH, Hagigeorges D, Manatis-Lornell AJ, Dommasch E, Senna MM. 2019. Hair loss among transgender and gender-nonbinary patients: a cross-sectional study. Br J Dermatol. 181:1082–1083.
33. Rocha VB, *et al.* 2018. Photopatch and patch testing in 63 patients with frontal fibrosing alopecia: a case series. Br J Dermatol. 179(6):1402–1403.
34. Bradding P, Pejler G. 2018. The controversial role of mast cells in fibrosis. Immunol Rev. 282(1):198–231.
35. Hobo A, *et al.* 2018. IL-17-positive mast cell infiltration in the lesional skin of lichen planopilaris: possible role of mast cells in inducing inflammation and dermal fibrosis in cicatricial alopecia. Exp Dermatol.29:273–277.
36. Jabbari A, *et al.* 2018. An open-label pilot study to evaluate the efficacy of tofacitinib in moderate to severe patch-type alopecia areata, Totalis, and Universalis. J Invest Dermatol. 138:1539–1545.
37. Mackay-Wiggan J, *et al.* 2016. Oral ruxolitinib induces hair regrowth in patients with moderate-to-severe alopecia areata. JCI insight. 1(15):e89790.
38. Yang CC, Khanna T, Sallee B, Christiano AM, Bordone LA. 2018. Tofacitinib for the treatment of lichen planopilaris: a case series. Dermatol Ther. 31(6):e12656.
39. Hermans MAW, *et al.* 2018. The JAK1/JAK2- inhibitor ruxolitinib inhibits mast cell degranulation and cytokine release. Clin Exp Allergy. 48(11):1412–1420.